Eur. Phys. J. C 34, 429–433 (2004)
Digital Object Identifier (DOI) 10.1140/epjc/s2004-01733-5

THE EUROPEAN PHYSICAL JOURNAL C

# QCD evolution and skewedness effects in color dipole description of DVCS

L. Favart[1,a], M.V.T. Machado[2,3,4,b]

[1] IIHE – CP 230, Université Libre de Bruxelles, 1050 Brussels, Belgium
[2] Instituto de Física e Matemática, Universidade Federal de Pelotas, Caixa Postal 354, CEP 96010-090, Pelotas, RS, Brazil
[3] High Energy Physics Phenomenology Group, GFPAE, IF-UFRGS, Caixa Postal 15051, CEP 91501-970, Porto Alegre, RS, Brazil
[4] CERN Theory Division. 1211 Genève 23, Switzerland

Received: 30 January 2004 / Revised version: 12 February 2004 /
Published online: 8 April 2004 – 

**Abstract.** We show the role played by QCD evolution and skewedness effects in the DVCS cross section at large $Q^2$ within the color dipole description of the process at photon level. The dipole cross section is given by the saturation model, which can be improved by DGLAP evolution at high photon virtualities. We investigate both possibilities as well as the off-forward effect through a simple phenomenological parameterization. The results are compared to the recent ZEUS DVCS data.

## 1 Introduction

An important clean process allowing us to access off-diagonal (skewed) parton distributions, which carry new information on the nucleon's dynamical degrees of freedom, is the deeply virtual Compton scattering (DVCS) process [1–3]. This is due to the real photon in the final state being an elementary (point-like) particle rather than a bound state like a meson or more complicated configurations. The skewed parton distributions are generally defined via the Fourier transform of matrix elements of renormalized, non-local twist-two operators (for a pedagogical view, see [4,5]). These composite operators contain only two elementary fields of the theory, which are placed at different positions becoming then non-local and operating in unequal momentum nucleon states.

Hence skewedness takes into account dynamical correlations between partons with different momenta. The high energy situation at HERA gives the important opportunity to constrain them as well as to study the evolution with virtuality of the resulting quark and gluon distributions. There are several representations for skewed parton distributions [6–10], which can be used to compute the relevant observables in DVCS (or other exclusive processes) through a factorization theorem [11]. They are input in numerical solutions of the renormalization group or evolution equations (see e.g. [12]), producing very reliable predictions up to NLO level [13]

On the other hand, the color dipole models have also been successful in describing DVCS observables [14–16]. There, the main degrees of freedom are the color dipoles, which interact with the nucleon target via gluonic exchange. This interaction is modeled through the dipole–nucleon cross section, which can include QCD dynamical effects given by DGLAP, BFKL or non-linear high energy evolution equations (parton saturation). Skewedness effects are not considered in the current dipole models, and this is one of the goals of the present analysis, making use of a simple phenomenological parameterization to estimate them. Moreover, the QCD DGLAP evolution can be introduced, which improves the data description in the large $Q^2$ kinematic region accessible in the recent ZEUS DVCS measurements [3].

This note is organized as follows. In the next section, we recall the main formulas for the color dipole formalism applied to DVCS. For the dipole cross section we have considered the saturation model [17], which produces a unified and intuitive description of DIS [17], diffractive DIS [18], vector meson production [19], Drell–Yan [20,21] and DVCS [16]. In particular, the restriction to the transverse part of the photon wave function, due to the real final state photon in DVCS, enhances the contribution of larger dipole configurations and therefore the sensitivity to soft content and to the transition between hard/soft regimes. Such a feature provides a particularly relevant test of saturation models. Moreover, the approach includes all twist resummation, in contrast to the leading twist approximations. In Sect. 3, we discuss the role played by the QCD evolution and skewedness in the high virtuality kinematic region. We also perform a systematic analysis in order to investigate to what extent the distinct models improve the data description. These issues have implications in the correct determination of the $t$ slope parameter $B$, whose value has never been measured for DVCS. Finally, the last section summarizes our main results.

[a] e-mail: lfavart@ulb.ac.be
[b] e-mail: magnus@if.ufrgs.br, magnus@ufpel.edu.br

## 2 DVCS cross section in dipole picture

In the proton rest frame, the DVCS process can be seen as a succession in time of three factorizable subprocesses:
(i) the photon fluctuates in a quark–antiquark pair;
(ii) this color dipole interacts with the proton target;
(iii) the quark pair annihilates in a real photon. The usual kinematic variables are the $\gamma^* p$ CMS energy squared $s = W^2 = (p+q)^2$, where $p$ and $q$ are the proton and the photon momenta respectively, the photon virtuality squared $Q^2 = -q^2$ and the Bjorken scale $x_{\rm Bj} = Q^2/(W^2+Q^2)$.

The imaginary part of the DVCS amplitude at zero momentum transfer in the color dipole formalism is expressed in the simple way [16],

$$\mathcal{I}\mathrm{m}\,\mathcal{A}\,(s, t=0) = \int_0^1 \mathrm{d}z \int_0^\infty \mathrm{d}^2\boldsymbol{r}\, H(z,\boldsymbol{r},Q^2)\,\sigma_{\rm dip}(\tilde{x},\boldsymbol{r}^2), \quad (1)$$

$$H = \frac{6\alpha_{\rm em}}{4\,\pi^2} \times \sum_f e_f^2 \,\left\{\left[z^2+(1-z)^2\right]\,\varepsilon_1\,K_1(\varepsilon_1\,r)\,\varepsilon_2\,K_1(\varepsilon_2\,r) + m_f^2\;K_0(\varepsilon_1\,r)\,K_0(\varepsilon_2\,r)\right\}\,, \quad (2)$$

where $H(z,\boldsymbol{r},Q^2_{1,2}) = \Psi^*_{\rm T}(z,\,\boldsymbol{r},\,Q_1^2=Q^2)\,\Psi_{\rm T}(z,\,\boldsymbol{r},\,Q_2^2=0)$, with $\Psi_{\rm T}$ being the light cone photon wave function for transverse photons. Here, $Q_1 = Q$ is the virtuality of the incoming photon, whereas $Q_2$ is the virtuality of the outgoing real photon. The longitudinal piece does not contribute at $Q_2^2 = 0$. The relative transverse separation of the pair (dipole) is labeled by $\boldsymbol{r}$ and $z$, $(1-z)$, are the longitudinal momentum fractions of the quark (antiquark). The auxiliary variables $\varepsilon^2_{1,\,2} = z(1-z)\,Q^2_{1,\,2}+m_f^2$ depend on the quark mass, $m_f$. The $K_{0,1}$ are the McDonald functions and summation is taken over the quark flavors.

Let us summarize the main features and expressions from the saturation model, which will be used here to estimate the DVCS cross section. A previous analysis compared to H1 data can be found in [16]. The saturation model reproduces color transparency behavior, $\sigma_{\rm dip} \sim \boldsymbol{r}^2$, for small dipoles, whereas it gives a constant behavior for large ones. This is rendered by a dipole cross section having an eikonal-like form,

$$\sigma_{\rm dip}(\tilde{x},\,\boldsymbol{r}^2) = \sigma_0\,\left[1-\exp\left(-\frac{Q^2_{\rm sat}(\tilde{x})\,\boldsymbol{r}^2}{4}\right)\right], \quad (3)$$

$$Q^2_{\rm sat}(\tilde{x}) = \left(\frac{x_0}{\tilde{x}}\right)^{\lambda}\,\mathrm{GeV}^2,\;\; \tilde{x} = x_{\rm Bj}\left(1+\frac{4\,m_f^2}{Q^2}\right), \quad (4)$$

where the saturation scale $Q_{\rm sat}(x)$ (energy dependent) defines the onset of the saturation phenomenon and sets the interface between soft/hard domains. The parameters were obtained from a fit to the HERA data producing $\sigma_0 = 23.03\,(29.12)\,\mathrm{mb}$, $\lambda = 0.288\,(0.277)$ and $x_0 = 3.04\cdot10^{-4}\,(0.41\cdot10^{-4})$ for a 3-flavor (4-flavor) analysis [17]. An additional parameter is the effective light quark mass, $m_f = 0.14\,\mathrm{GeV}$. For the 4-flavor analysis, the charm quark mass is considered to be $m_c = 1.5\,\mathrm{GeV}$.

The QCD evolution to the original saturation model was implemented recently [22] (BGBK), where the dipole cross section now depends on the gluon distribution in a Glauber–Gribov inspired way,

$$\sigma_{\rm dip}\,(\tilde{x},\boldsymbol{r}^2) = \sigma_0\left[1-\exp\left(-\frac{\boldsymbol{\pi}^2\,\boldsymbol{r}^2\,\alpha_{\rm s}(\mu^2)\,\tilde{x}\,G(\tilde{x},\mu^2)}{3\,\sigma_0}\right)\right], \quad (5)$$

where the energy scale is defined as $\mu^2 = C/\boldsymbol{r}^2 + \mu_0^2$. The parameters are determined from a fit to the DIS data, with the following initial condition for LO DGLAP evolution: $x\,G(x,\mu^2=1\,\mathrm{GeV}^2) = A_g\,x^{-\lambda_g}\,(1-x)^{5.6}$. The flavor number is taken to be equal to 3. The overall normalization $\sigma_0 = 23.03\,\mathrm{mb}$ is kept fixed (labeled fit 1 in [22]). The DGLAP evolution improves the data description in the large $Q^2$ regime and brings the model close to the theoretical high energy non-linear QCD approaches.

Having a suitable model for the dipole cross section, as in (3) or (5), we can use (1) and then compute the final expression for the DVCS cross section:

$$\sigma(\gamma^*\,p\to\gamma\,p) = \frac{1}{B}\,\frac{\left[\,\mathcal{I}\mathrm{m}\,\mathcal{A}(s,0)\,\right]^2}{16\,\boldsymbol{\pi}}\,\left(1+\rho^2\right), \quad (6)$$

where $B$ is the $t$ slope parameter (the behavior in $|t|$ is supposed to obey a simple exponential parameterization).

In our further calculations, the real part is included via the usual estimate $\rho = \tan(\boldsymbol{\pi}\lambda/2)$, where $\lambda = \lambda(Q^2)$ is the effective power of the imaginary part of the amplitude. We have fitted it for $1 \le Q^2 \le 100\,\mathrm{GeV}^2$ in the form $\lambda_{\rm eff}(Q^2) = 0.2+0.0107\ln^2(Q^2/2.48)$. It can be verified that when it rises to $\sim 0.3$ at high virtualities the contribution of the real part can reach 20% of the total cross section. In the next section we compute the cross section above using the two versions for the saturation model and contrast them with the recent DVCS ZEUS data, which includes data points with larger $Q^2$ values than the previous H1 data. Moreover, we present a simple way to introduce the skewedness effects into the calculation.

## 3 Results and discussions

In Fig. 1 is shown the result for the saturation model, see (3), confronted to the experimental data on DVCS of recent ZEUS measurements as a function of the CMS energy, $W_{\gamma p}$ (at fixed virtuality $Q^2 = 9.6\,\mathrm{GeV}^2$). The parameters of the 4-flavor fit have been used, producing good agreement with a fixed value for the slope, $B = 4\,\mathrm{GeV}^{-2}$.

In Fig. 2a, we show the result of the saturation model for the behavior with $Q^2$ at fixed energy, $W_{\gamma p} = 89\,\mathrm{GeV}$. In order to illustrate the sensitivity on the slope value, both values $B = 4\,\mathrm{GeV}^{-2}$ (solid line) and $B = 6.5\,\mathrm{GeV}^{-2}$ (dot-dashed line) are shown[1]. Although the statistical errors are large, it seems that for $Q^2 \gtrsim 40\,\mathrm{GeV}^2$, the model

[1] It is worth mentioning that a slope $B = 6.5\,\mathrm{GeV}^{-2}$ (4-flavor) was able to describe correctly the H1 experimental data for $Q^2 \le 40\,\mathrm{GeV}^2$ [16].

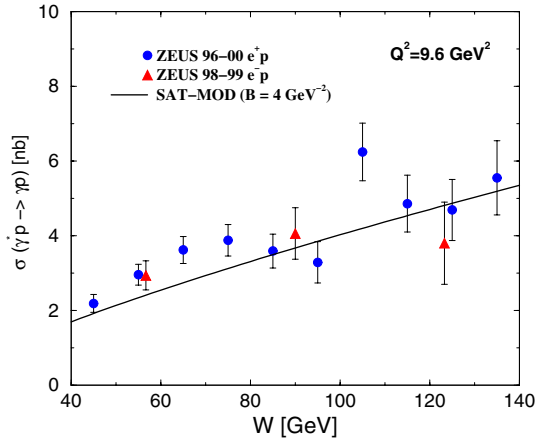


**Fig. 1.** The DVCS cross section as a function of CMS energy, $W_{\gamma p}$. The curve is the result for the saturation model for fixed slope $B = 4\,\mathrm{GeV}^{-2}$

underestimates the experimental data. This can indicate two things:
(a) the slope diminishes as the virtuality increases or,
(b) some additional effect appears at higher $Q^2$.

In order to investigate the first hypothesis, we compute the cross section using a $Q^2$-dependent slope, proposed in [23]. That is, $B(Q^2) = B_0\,[1 - 0.15\ln(Q^2/2)]\,\mathrm{GeV}^{-2}$ which is based on the diffractive electroproduction of $\rho$. Such a slope dependence allows a good description of the $Q^2$ dependence of the cross section up to the highest measured values and gives a good normalization for $B_0 = 5\,\mathrm{GeV}^{-2}$.

In order to investigate whether a QCD evolution improves the description, we show in Fig. 2b the estimate using the BGBK dipole cross section, (5) as a function of $Q^2$ using fixed slope values. There is an effect in the overall normalization and a slower decrease at large $Q^2$ in contrast with the model without QCD evolution reproducing well the ZEUS measurement for all $Q^2$. This suggests that DGLAP evolution starts to be important for the large $Q^2$ points measured by ZEUS. A comparison of the different $Q^2$ behavior independently of the normalization question is presented at the end of this section.

Furthermore, we are motivated to investigate the importance of the skewedness effects in the DVCS process using the previous results. Here, we follow the approximation proposed in [24], where the ratio of off-forward to forward parton distributions are obtained relying on simple arguments. The behavior of those ratios are given explicitly by [24],

$$R_{q,g}\,(Q^2) = \frac{2^{2\lambda+3}}{\sqrt{\pi}}\,\frac{\Gamma\left(\lambda+\frac{5}{2}\right)}{\Gamma\,(\lambda+3+p)}\,, \qquad (7)$$

where $p = 0$ for quarks and $p = 1$ for gluons, and where $\lambda$ is the exponent of the $x^{-\lambda}$ behavior of the input diagonal parton distribution. It should be noticed that the skewed effect is much larger for singlet quarks than gluons. In the following, it will be assumed that the DVCS cross section is lead by a two gluon exchange. In our further computations, we use $\lambda = \lambda(Q^2)$ as discussed in the previous section, and the skewedness effect is given by multiplying the total cross section by the factor $R_g^2(Q^2)$. Once the effective power increases as a function of $Q^2$, the skewedness effects could enhance the cross section by a factor two if values of $\lambda_{\mathrm{eff}} \simeq 0.4$ are reached at larger virtualities. In Fig. 3a we show the result using the saturation model (4-flavor) and the skewedness correction; see (7). The same analysis is shown for the BGBK model in Fig. 3b. The main effect is to increase the overall normalization of the cross section by about 40% and only slightly modify the large $Q^2$ behavior. Again, this will be shown more clearly and independently of the normalization at the end of this section.

For completeness, we have investigated two additional versions of the implementation of the skewedness correction factor. They are shown in Fig. 4 for fixed $B = 4\,\mathrm{GeV}^{-2}$. First, we have imposed the skewedness correction only for small dipoles by introducing $R_g(\lambda_{\mathrm{GBW}} = 0.277)$ in the exponent of (3) (dotted line). This is to prevent correction to the non-perturbative (large dipoles) piece of the dipole cross section. Further, we also test the rough approximation $\tilde{x} = 0.41\,x_{\mathrm{Bj}}$ (dashed line), which comes from a simplified hypothesis, $\sigma_{\mathrm{dip}} \sim R_g(\lambda)\;(x_{\mathrm{Bj}})^{-\lambda}$. The conclusion is that these two different implementations of the skewedness correction do not make sensible changes with respect to the first skewedness correction neither in the normalization nor in the $Q^2$ dependence for the presently covered kinematic range and precision of the measurement.

At this stage, some comments are probably needed. The estimate for the skewedness taken into account above is an approximation, as we currently have no accurate theoretical arguments how to compute it from first principles within the color dipole formalism. A consistent approach would be to compute the scattering amplitude in the non-forward case (the non-forward photon wave function has been recently obtained in [25]). In this case, the dipole cross section, $\sigma_{\mathrm{dip}}(x_1, x_2, \boldsymbol{r}, \boldsymbol{\Delta})$, depends on the light cone momenta $x_1$ and $x_2$ carried by the exchanged gluons, respectively, and on the total transverse momentum transfer $\boldsymbol{\Delta}$ (additional information on the behavior on $\boldsymbol{\Delta}$ is needed for the QCD pomeron and proton impact factor). The forward dipole cross section is recovered at $x_1 = x_2$ and $\boldsymbol{\Delta} = 0$. In the future, an experimental constraint for the non-forward dipole cross section should be feasible with increasing statistics on DVCS and exclusive (diffractive) vector meson production.

To close this section: as the slope parameter $B$ has never been measured for DVCS, we compare the different estimates presented in a systematic way separately for the effect on the $Q^2$ dependence and the effect on the overall normalization. To compare the $Q^2$ dependences, we normalize all models to describe the ZEUS data point at the lowest $Q^2$ value, i.e. $Q^2 = 7.5\,\mathrm{GeV}^2$. Further, we plot the ratio of each model to our baseline model SAT-MOD as a function of $Q^2$. Such a procedure allows a $Q^2$ dependence comparison independently of the normalization effect. These ratios are shown in Fig. 5a, where the points (triangles-up) are the ratio of the ZEUS data to SAT-MOD including the error bars for the statistical (inner) and sum in quadrature of statistical and systematic (outer) uncertainties.

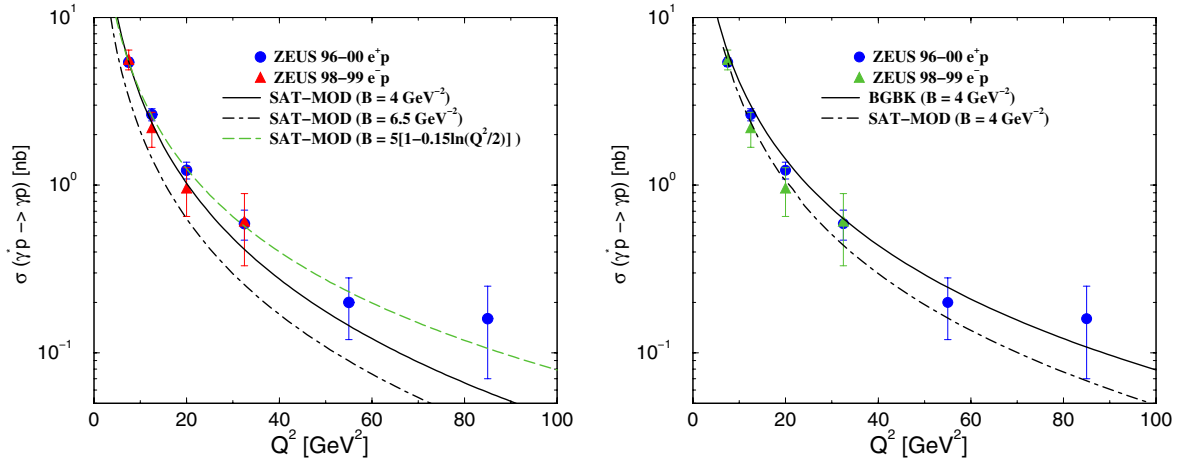


**Fig. 2.** The DVCS cross section as a function of photon virtuality: **a** saturation model using $B = 4$ and 6.5 $\mathrm{GeV}^{-2}$ (solid and dashed curves) and $Q^2$-dependent slope (dot-dashed curve – see text). **b** Effect of the BGBK model (includes QCD evolution) using $B = 4\,\mathrm{GeV}^{-2}$ (solid and dot-dashed curves)

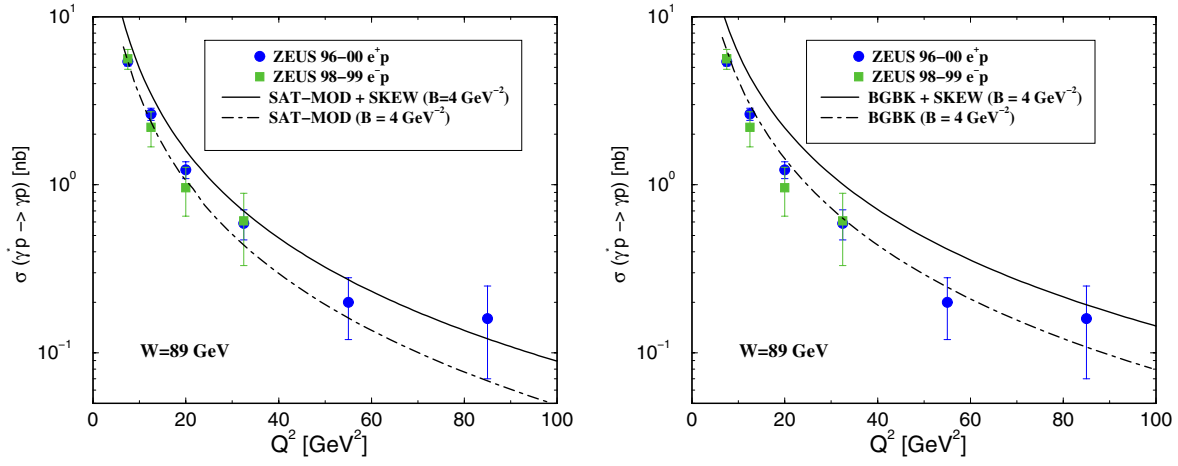


**Fig. 3.** The results for the **a** saturation model with (full) and without (dot-dashed) skewedness effect and **b** BGBK model, with (dot-dashed) and without (full) skewedness effect for a fixed $B = 4\,\mathrm{GeV}^{-2}$

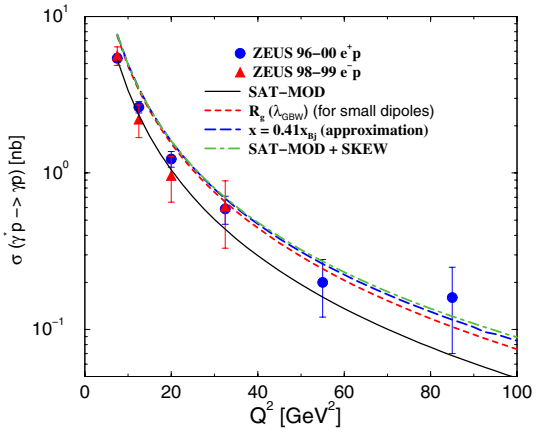


**Fig. 4.** Comparison among different approximations for the skewedness correction (see text)

On the other hand, to compare the effect on the normalization we show the slope value needed to describe the lowest $Q^2$ value of the ZEUS data points $B_0 = B(Q^2 = 7.5\,\mathrm{GeV}^2)$. They are shown in Fig. 5b. For completeness, we also present the measured slope values for vector meson production at that virtuality, both for $\rho^0$ and $J/\Psi$ mesons as indications of typical values for respectively light and heavy mesons using the simple parameterization:

$$B = 0.60 \left( \frac{14}{(Q^2 + M_V^2)^{0.26}} + 1 \right), \qquad (8)$$

where $M_V$ is the meson mass.

From these comparisons, we conclude that several models can account for the measured $Q^2$ dependence (SAT-MOD+B($Q^2$), SAT-MOD+SKEW and BGBK, as well as combination of several of those effects) which are not distinguishable with the present experimental precision. The difference between the models is much more pronounced

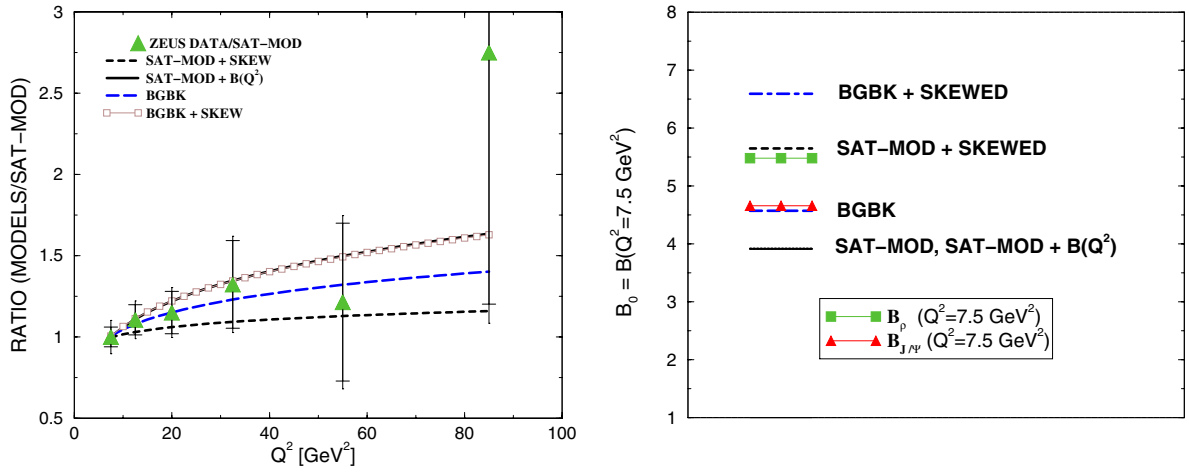


(a) (b)

**Fig. 5.** The ratio **a** MODELS/SAT-MOD as a function of $Q^2$ (models normalized to ZEUS data at $Q^2 = 7.5\,\mathrm{GeV}^2$) and **b** slope values of the models at $Q^2 = 7.5\,\mathrm{GeV}^2$ and slopes of heavy and light vector mesons

in the prediction of the cross section value, or in other terms, in the $B$ value needed to describe the integrated cross section over the available $Q^2$ range. If the change in normalization is small for the inclusion of a $Q^2$ dependence in $B$, the effect is of the order of 12% for BGBK with respect to the basic SAT-MOD and of 40% for the skewedness effect (SKEW) and still larger when the different effect are combined (60% for BGBK+SKEW).

In summary, these issues show clearly the importance of a measurement of the $t$ slope parameter $B$.

## 4 Summary

It has been shown that the DVCS cross section at HERA can be described by the simple picture rendered by the color dipoles formalism. In particular, the saturation model does an excellent job in the current experimental kinematic domain. To achieve a good description of the data up to the highest $Q^2$, the original saturation model can be supplemented by a QCD evolution, an additional dependence of $B$ on $Q^2$ and skewedness effects. These effects modify in a sensitive way the absolute cross section (10–60%). Measurement of the $t$ slope parameter $B$ would already allow one to discriminate among the different theoretical predictions with an amount of data comparable to the present ZEUS measurement.

*Acknowledgements.* M.V.T.M. thanks the CERN Theory Division, where part of this work was performed, for the hospitality and financial support. The work of L. Favart is supported by the FNRS of Belgium (convention IISN 4.4502.01) and M. Machado was partially financed by the Brazilian funding agency CNPq.

## References

1. C. Adloff et al. [H1 Collaboration], Phys. Lett. B **517**, 47 (2001)
2. L. Favart, Studies of DVCS and photoproduction of photons at high t with the H1 detector, in International Europhysics Conference on High Energy Physics (EPS03), July 17–23, Aachen (2003) [hep-ex/0312013]
3. S. Chekanov et al. [ZEUS Collaboration], Phys. Lett. B **573**, 46 (2003)
4. A. Freund, Eur. Phys. J. C **31**, 203 (2003)
5. M. Diehl, Phys. Rept. **388**, 41 (2003)
6. D. Müller et al., Fortschr. Phys. **42**, 101 (1994)
7. X. Ji, Phys. Rev. D **55**, 7114 (1997)
8. A.V. Radyushkin, Phys. Rev. D **56**, 5524 (1997)
9. K.J. Golec-Biernat, A.D. Martin, Phys. Rev. D **59**, 014029 (1999)
10. L. Frankfurt et al., Phys. Lett. B **418**, 345 (1998), Erratum **429**, 414 (1998); A. Freund, V. Guzey, Phys. Lett. B **462**, 178 (1999)
11. J.C. Collins, A. Freund, Phys. Rev. D **59**, 074009 (1999)
12. A. Freund, M. McDermott, Phys. Rev. D **65**, 074008 (2002)
13. A. Freund, M. McDermott, Phys. Rev. D **65**, 056012 (2002); Phys. Rev. D **66**, 079903 (2002); Phys. Rev. D **65**, 091901 (2002); Eur. Phys. J. C **23**, 651 (2002)
14. A. Donnachie, H.G. Dosch, Phys. Lett. B **502**, 74 (2001)
15. M. McDermott, R. Sandapen, G. Shaw, Eur. Phys. J. C **22**, 655 (2002)
16. L. Favart, M.V. Machado, Eur. Phys. J. C **29**, 365 (2003)
17. K. Golec-Biernat, M. Wusthoff, Phys. Rev. D **59**, 014017 (1999)
18. K. Golec-Biernat, M. Wusthoff, Phys. Rev. D **60**, 114023 (1999)
19. A.C. Caldwell, M.S. Soares, Nucl. Phys. A **696**, 125 (2001)
20. M.A. Betemps, M.B. Gay Ducati, M.V. Machado, Phys. Rev. D **66**, 014018 (2002)
21. M.A. Betemps, M.B. Ducati, M.V. Machado, J. Raufeisen, Phys. Rev. D **67**, 114008 (2003)
22. J. Bartels, K. Golec-Biernat, H. Kowalski, Phys. Rev. D **66**, 014001 (2002)
23. A. Freund, M. McDermott, M. Strikman, Phys. Rev. D **67**, 036001 (2003)
24. A.G. Shuvaev, K.J. Golec-Biernat, A.D. Martin, M.G. Ryskin, Phys. Rev. D **60**, 014015 (1999)
25. J. Bartels, K. Golec-Biernat, K. Peters, Acta Phys. Polon. B **34**, 3051 (2003)